Indonesian Journal of Electrical Engineering and Computer Science
Vol. 28, No. 2, November 2022, pp. 898~908
ISSN: 2502-4752, DOI: 10.11591/ijeecs.v28.i2.pp898-908

Computer modeling and simulation to predict COVID-19 propagation patterns via factual cellular automata

Shahinaz M. Al-Tabbakh[1], Marwa A. Karim[2]
[1]Computer Sciences and Applications-Physics Department, Faculty of Women for Arts, Sciences and Education, Ain Shames University, Cairo, Egypt
[2]Ophthalmology Department, Faculty of Medicine, Ain Shames University, Cairo, Egypt

Article Info

Article history:

Received Aug 28, 2021
Revised Jul 29, 2022
Accepted Aug 16, 2022

Keywords:

Cellular automata
Computer modeling
COVID-19
Epidemic propagation
Simulation

ABSTRACT

Computer modelling and simulation methods are very important and play a critical role in the mitigation and response to the ongoing COVID-19 pandemic. In this study, we propose a computational modeling technique based on cellular automata (CA) with realistic proposed rules. The rules are designed to simulate the propagation of COVID-19 disease through a bounded area. Our proposed CA rules are novel in many respects. For example, we introduce rules regarding surface states not only the states of the person rules to the proposed model. In addition on, the classification of neighbors to nearest neighbors and range of neighbors based on cellular layers is explained. Moreover, the concepts of time generation and access time are deployed for the first time to model the propagation of the disease over time in this work. Further details of the proposed model including the topology of the defined area, the initial states of the cells and four-layer transfer mechanism are explained as well. This work may be considered a criterion of spreading for COVID-19 from point source in a defined population area. The results of the proposed algorithm represent the percentage of the population whose infectious status is described by different cellular state objects after a defined generation time. The results are compared under different circumstances and analyzed equanimity.

Corresponding Author:

Shahinaz. M. Al-Tabbakh
Department of Physics, Faculty of Women for Arts, Sciences and Education, Ain Shames University
Cairo Governorate, Egypt
Email: shahinaz.altabbakh@women.asu.edu.eg

1. INTRODUCTION

COVID-19 seems to have become a major worldwide concern as one of the strongest infectious disease epidemics currently, with a death toll exceeding five million people globally. The disease is highly infectious being transmitted from person to person through close contacts, via respiratory droplets and aerosolized particles produced by infected person during any exhalation, especially coughing or sneezing [1]. The SARS-COV2 virus the causative agent of this disease, tends to infect the respiratory system, leading to a range of outcomes from cold like symptoms to pneumonia, cold, sneezes and coughing. In situations of severe infection, it has caused upper respiratory illnesses, kidney dysfunction, diarrhea, and heart damage [2]. On the other hand, the globalization of the COVID-19 pandemic and its economic consequences to cause economic disruption and dislocation throughout the world, sending many economies into steep recessions or depressions. As the number of infected people and deaths rise, global recovery from the pandemic remains uncertain, based on existing statistics declared for COVID-19 pandemic. Even economies of the developed

countries such as those of Europe, as well as the United States have been already affected by the COVID-19 crisis [3].

Computational modeling is an efficient tool in the struggle against the COVID-19 pandemic because modeling approaches able to observe in depth the characteristics of pathogens in details and effort to predict its behavior over long period of time [4], [5]. In general, differential equations, Poisson's equation [6], LaPlace's equation, and Maxwell's equations [7], [8] have been used to model all epidemics. These methods can solve some complex and dynamic propagation problems. However, these approaches involve some serious drawbacks and thus tend to neglect the local character of the propagation of each epidemic [9], [10]. Most current causeways do not allow for individual differences and do not consider the complicated boundary and start up conditions. Cellular automata (CA) modeling techniques can overcome the aforementioned drawbacks and have been employed as an alternate method of epidemics modelling by various savants [11], [12]. CA as well prove to be a better alternative of usage under specific boundary and preliminary conditions in solving the scientific problems associated to partial differential equations [13]. The nature of cellular automata, which abstracts the system's global behavior from the interactions of local cells, makes it a better alternative solution for estimating epidemic spread than differential equations. CA modeling technique is adapted to stochastic systems that exhibit simultaneous variation with space and time [14], [15].

In this paper, a practical model is proposed that based on a Cellular Automata technique, which can be employed to mimic the spread of coronavirus disease COVID-19 for different topologies and situations. The reminder of this work is organized as follows, section 2 introduces the related work model, and the proposed) model, named MAD-COV19, is presented in section 3. In section 4, results obtained from simulations are presented and analyzed to demonstrate the effectiveness of the proposed approach. In section 5, we present our conclusions in context and discuss the possible relevance of the proposed approach to existing efforts to model and predict the course of the pandemic.

2. THE COMPREHENSIVE THEORETICAL BASIS

Duan *et al.* [5] classify epidemic modeling to mathematical and computational approaches. These approaches play an essential role in understanding epidemic spread patterns and assessing disease control strategies. According to duan classification, the computational approaches in turn can be classified as agent based model and complex network models. Mathematical models can be classified as deterministic or stochastic. In deterministic epidemic modeling approach, the population is assumed to be homogenous, well-mixed and aggregated into small set of states. Transitions of the population between different states are formulated using differential equations with different factors such as infection rate, onset rate of symptoms, and recovery rate. Due to the variance in epidemic progress of different diseases, infected individuals may be categorized with a variety of healthy-state models. Two types of state models have been primarily proposed in the literature namely, susceptible, infected and recovered (SIR) and susceptible, infected (SI).

Keeling and Danon [14] represented SIR, which has become a most important generic mathematical model. This model concentrated on classifying the population into three classes. Those are susceptible (S), infected (I) and recovered (R). The traditional SIR model is represented as (1), and (2) [5].

$$\frac{dS(t)}{\partial t} = -fs(t)i(t), \quad (1)$$

$$\frac{di(t)}{\partial t} = -fs(t)i(t) - r\,i(t) \quad (2)$$

The susceptible individuals are the ones who can catch the disease; while the infected people are those who can spread the disease, and the recovered people are those who are resistant to the disease, whether by the virtue of surviving the disease and recovering or because of their natural immunity concerns. When susceptible individuals are infected by an epidemic with infection rate (f), they are considered to fall into the infected states. Meanwhile, infectious individuals can transmit the epidemic. After the infectious period, infected individuals are then in a recovered state with recovery rate (r) and become immune to the epidemic.

In the SI model, the population is divided into two classes, including the susceptible individuals who may contract the disease and infected individuals who may spread the disease to susceptible persons [14]. When a susceptible person becomes infected, he is transferred to the infected class, increasing the count of the infected class while decreasing the count of susceptible. The SI model supposes that each person in the vulnerable population has an equal chance of contracting the disease through interaction with an infected individual. Once infected, a person cannot recover; they are livelong assigned to the I class [16]. Allen [17] assumed that the length of the disease outbreak modeled to be short compared with an average person's lifespan. This framework is developed to consider a spatial or indoor domain over a limited time period. Therefore, this model can be applied to diseases from which individuals never recover and the spread is

relatively rapid, such as herpes caused by the virus Herpesviridae, and COVID-19 caused by SARS-COV2 virus in a spatial domain. The count of individuals in the susceptible and infective populations at time (n+1) Δt in the SI epidemic model with discrete time can be described by the two difference equations:

$$S_{n+1}=S_n\left(1-\frac{\propto\Delta t}{N}\right)I_n \quad (3)$$

$$I_{n+1}=I_n\left(1+\frac{\propto\Delta t}{N}\right)S_n \quad (4)$$

where Δt is the fixed time step, N is the total size of the population, and α is the ratio of contact between the susceptible and infectious agents that enables the susceptible to become infected per unit time. The time step Δt should be shorter than the mean transmission time.

The beginning conditions for disease progression are given by S_0 and I_0, the count of susceptible and infected individuals at time n = 0. With the assumption that $S_0 + I_0 = N$ with $0 \leq S_0 \leq N$ and $0 \leq I_0 \leq N$. The non-discretized SI model includes two equilibrium points. The first one is (N, 0), which denotes there have never been any infected individuals, as well as the second is (0, N), that denotes, the entire population becomes diseased [15].

The parameter is given as the rate of infection so that the continuous analogues (3) and (4) may be readily derived. Using the approximation, $(S_{n+1}-S_n)/\Delta t=ds/dt$, the analogous differential equations has the following form [15]:

$$\frac{dS(t)}{dt}=-\frac{\propto}{N}SI \quad (5)$$

$$\frac{dI(t)}{dt}=\frac{\propto}{N}SI \quad (6)$$

the solution of the continuous model can be obtained exactly from [15].

$$I(t)=\frac{I(0)N}{[I(0)+\exp(-\propto t)(N-I(0))]} \quad (7)$$

Substituting N-1 for S in the SI differential equation model yields a logistic differential equation (5) in which I(t) approaches N monotonically. The continuous model exhibits the same behavior as the discrete model. The spread of infectious diseases can be characterized well in a non-uniform field using cell-based models namely, cellular automata (CA). Instead of the complicated solution methods for differential equations described in the relevant literatures, CA models have been successfully solved by tracking the number of cells along a time evolution. White et al. offered a deterministic model derived from the cellular automata to mockup the dissemination of an outbreak of an epidemic disease [18]. In the model, individuals are assumed to be dispersed in the cellular space within two shapes. In the first shape, each cell holds for an individual in the population whereas in the second shape, each cell includes several individuals instead of a single one to simulate large zones. However, White *et al.* [18] considered three classes of population, including susceptible, infected, and recovered. Sirakoulis *et al.* [19] demonstrated that the distance of movement and the count of individuals moving are the two most significant parameters, which are taken into interest by their set of rules. Dascălu *et al.* [20] presented a cellular automaton model to examine the effects of inhabitants' movement and vaccination on epidemic propagation. The model assumed that each cellular automaton cell denotes a part of the total population that may be found in one of three states: infected, immunized, and susceptible. They explored the effect of the two factors of population movement parameters on the spread of epidemics namely, the distance of movement and the percentage of the inhabitants moving. Furthermore, their model was augmented to include the effect of vaccination on epidemic spread in some parts of the population. Their model exhibits an accurate epidemic disease because of the increase in the percentage of the population moving, or of the maximum distance of population movement. They also modeled that the effect of population vaccination in reducing the propagation percentage of epidemic. Dascalu et al. presented an enhanced cellular automaton modeling autonomous agent, to simulate the evolution of the spread of COVID-19 [20]. They conducted simulations that showed that the combination of cellular automata with autonomous agents can be used to successfully modeling the evolution of this disease, due to its sensitivity to factors associated with processes of infection and restoration. They introduced some improvements for their model including considering the topography of the space, a timer associated with each autonomous agent to model their change of state (and the testing strategies), a FIFO memory designed

to model the treatment facilities, and the global control of the system by various law enforcement groups and governmental authorities. Dai *et al.* [21] presented a cellular automats model designed to analyze the evolution of COVID-19 epidemic. A simplified physical social community is simulated and expressed on a two-dimensional plane. Individual heterogeneity parameters were considered including sex ratio, age, individual immunity, treatment period, and population movement, but object infections, effects of vacant spaces and congestion were not included. Also, the authors adapted COVID-19 confirmation data from New York City and Iowa to validate purposes of that study.

Jithesh build up a probabilistic cellular automata model designed to estimate the peak and duration of COVID-19 propagation in a cluster under various situations. The two-dimensional CA arrangement was applied as a regular lattice that represents a population subset, with each cell representing a person in a specific stage. A transition table and transmission neighborhoods were developed around each single cell. The transition rule asserts that virus transmission happens when susceptible individuals are present in the infected individual's transmittable area, which breaches the conditions of social isolation. The model parameters such as the size of the susceptible population, the range of the neighborhood, and various illness features the pandemic's time trajectory was simulated. The impact of migration and lockdown policies on the dynamics of the pandemic were also studied in this search [22]. Cárdenas *et al.* [23] developed a system simulator named a Cell-DEVS to imitate and investigate the spread of disease, focusing on the COVID-19 pandemic. Cell-DEVS [24] combines CA with discrete event system specifications (DEVS) to describe n-dimensional cell spaces as discrete-event models. Cárdenas *et al.* [23] applied SIR and SIER models on the simulator. The simulation language was explained also in this work [23],[24]. In general, the existing research on computer modelling and simulation of COVID-19 propagation documented in the relevant literature is still restricted and unresolved. As a result, this research is unique in that it predicts the spread of this disease in a restricted area with precise characteristics. The proposed cellular automata rules are intended to be realistic and to be consistent with COVID-19 data in order to clarify future possibilities. This study is groundbreaking in that it proposes guidelines for both surface states and the states of persons to be evaluated. The suggested model introduces the concept of cellular layers around each current cell to represent the nearest neighbors or range of neighbors. In the following part, the ideas of generation time and access time for modelling disease propagation are also created and discussed. To the best of our knowledge, this is the first study to look into the latter two areas.

3. METHOD

The features of the proposed modelling algorithm that explain the propagation of COVID-19 can be described as follows. The area of virus propagation under study is square matrix of size (L+10) x(L+10) units or cells. The boundary area is taken into consideration so that the actual area of propagation is L^2 cells. Each cell represents either an infected person or a susceptible person or either a contaminated surface or a cleared surface or vacant space. Each cell region represents the unit length of the area under consideration.

Each person cell in our proposed model may represent a person that carries the SARS-COV2 virus, or a person who doesn't carry the virus. The carrier may be in an exposed state (EX) or in infected state (INF). Persons in the infected state (INF) are taken in to consideration only in our proposed model, whereas a person not carrying the virus may be in a susceptible state (SUS) or recovered (R). The susceptible state (SUS) is taken in to consideration only in our model. Each surface cell may carry the SARS-COV2 virus, and are thus referred to as contaminated (CO) or cleared (CL), indicating that they no longer carry the virus. It is assumed that eight nearest neighbors in a two-dimensional plane encircle each cell, and the interaction rule with the neighbors is expressed by a transition matrix N where N represents the Moore's neighborhood of A (i, j) [25]. For each individual cell, the transition rules for A (i, j) are also inspired by the range neighbor up to four layers around the cell A (i, j) namely R. The classification of neighbors for cell A is defined in Figure 1. Figure 1(a) represents Moore's neighborhood (N) which is the first layer that encircle the cell A. Figure 1(b) illustrate the range of neighbors up to four layers around the cell A namely R.

The access times of all cells of the matrix were created randomly and inserted in a queue. Spreading time is referred to as the generation time. The generation time is a multiple of generation periods. The generation period is the period in which each cell in the area takes the opportunity to operate according to access time in a semi parallel approach with each neighbor. The operation of an individual cell is the ability of this cell in its infection state to transfer the virus to all its nearest neighbors in the next four cellular layers or to move to any vacant space in the first or second layer. Also, the operation of surface cells is the ability of this cell in its contamination state to transfer the virus agent to all nearest neighbors in the first cellular layer. Moreover, each cell should have its own access time in each generation period. The access times of all cells of the matrix were created randomly with uniform distribution and inserted in the queue. All cell regions of the matrix have a unique ID. The cell regions are sorted dynamically according to access times and inserted in another separate priority vector namely, regions. In other words, each cell should have its own access time in each generation

period. The cell region which has the least access time would operate first in its generation period. The access times for this technique of modeling is developed to guarantee the fairness of the current propagation model. The representation of the sorted access times through each generation period is shown in Figure 2.

A(i - 1, j - 1)	A(i - 1, j)	A(i - 1, j + 1)
A(i, j - 1)	A(i, j)	A(i, j + 1)
A(i + 1, j - 1)	A(i + 1, j)	A(i + 1, j + 1)

(a)

A(i-4,j-4)	A(i-4,j-3)	A(i-4,j-2)	A(i-4,j-1)	A(i-4, j)	A(i-4,j+1)	A(i-4,j+2)	A(i-4,j+3)	A(i-4,j+4)
A(i-3,j-4)	A(i-3,j-3)	A(i-3,j-2)	A(i-3,j-1)	A(i-3, j)	A(i-3,j+1)	A(i-3,j+2)	A(i-3,j+3)	A(i-3,j+4)
A(i-2,j-4)	A(i-2,j-3)	A(i-2,j-2)	A(i-2,j-1)	A(i-2, j)	A(i-2,j+1)	A(i-2,j+2)	A(i-2,j+3)	A(i-2,j+4)
A(i-1,j-4)	A(i-1,j-3)	A(i-1,j-2)	A(i-1,j-1)	A(i-1, j)	A(i-1,j+1)	A(i-1,j+2)	A(i-1,j+3)	A(i-1,j+4)
A(i,j-4)	A(i,j-3)	A(I,j-2)	A(i,j-1)	A(i,j)	A(i, j + 1)	A(i, j + 2)	A(i, j + 3)	A(i, j + 4)
A(i+1,j-4)	A(i+1,j-3)	A(i+1,j-2)	A(i+1,j-1)	A(i+1,j)	A(i+1,j+1)	A(i+1,j+2)	A(i+1,j+3)	A(i+1,j+4)
A(i+2,j-4)	A(i+2,j-3)	A(i+2,j-2)	A(i+2,j-1)	A(i+2,j)	A(i+2,j+1)	A(i+2,j+2)	A(i+2,j+3)	A(i+2,j+4)
A(i+3,j-4)	A(i+3,j-3)	A(i+3,j-2)	A(i+3,j-1)	A(i+3,j)	A(i+3,j+1)	A(i+3,j+2)	A(i+3,j+3)	A(i+3,j+4)
A(i+4,j-4)	A(i+4,j-3)	A(i+4,j-2)	A(i+4,j-1)	A(i+4,j)	A(i+4,j+1)	A(i+4,j+2)	A(i+4,j+3)	A(i+4,j+4)

(b)

Figure 1. The classification of neighbor region for each cell A (i, j), (a) N is Moore's neighborhood for A (i, j) and (b) R is the range of neighbors for cell A (i, j)

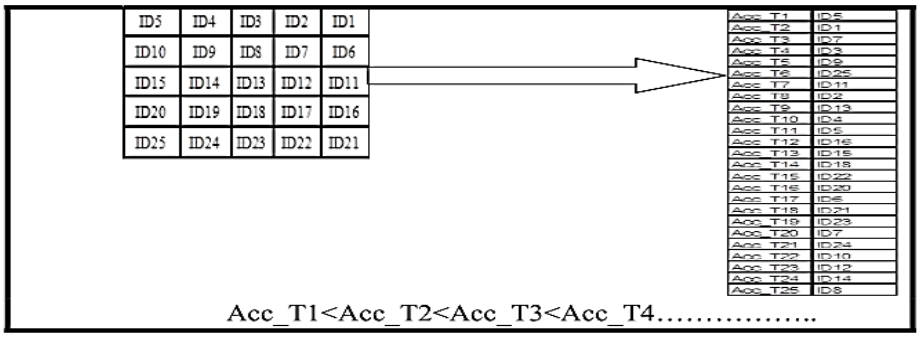

Figure 2. Representation of the access time queue and priority queue regions

The proposed model assumes that the SARS-COV2 virus is transferred from any cell with an INF state (infected person) to the range of neighbors (R) with different probabilities. In other words, if any one of nearest neighbor cells (N) is in a CL (cleared surface) state or SUS state (susceptible person), the move occurs with a probability 100%. The epidemic virus transfers to the second layer neighbors from the current cell with INF state with possibility 75% and to the third layer neighbors with probability 50%. The epidemic transfer to the fourth layer neighbors with probability 25%. Also, each person cell either SUS state or INF state can be moved or replaced by probability 50% if there are unfilled spaces around it in eight nearest neighbors (N). If the cell is vacant and surrounded by SUS or INF person, it can be replaced with INF individuals with probability 20% or SUS Individuals with probability 40% or remain in vacant space with probability 40%. If the current cell state is CO (contaminated surface), there is transfer of the virus agent from CO to its neighborhood (N) if any one of them is CL or SUS with probability 100%. Virus agents transfer only from CO cell to neighborhood (N) because of the touching possibility from the contaminated surface. Figure 3 represent the simple transfer rules through N. Figure 4 is the flowchart diagram for the proposed propagation algorithm.

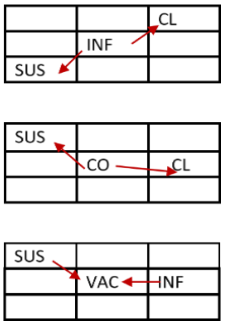

Figure 3. Illustration of the proposed cellular rules

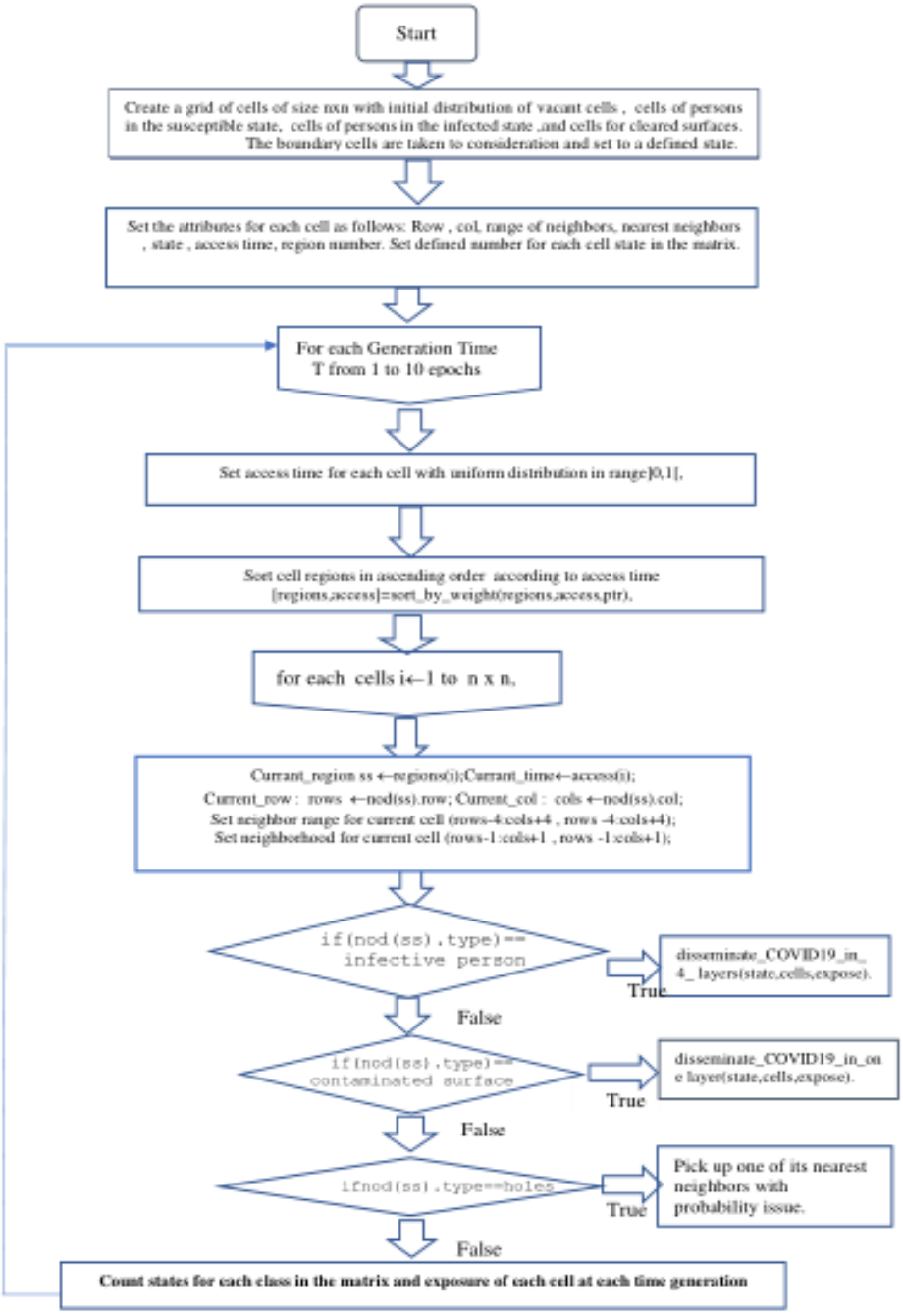

Figure 4. Flow chart plan for computer modeling system of dissemination of COVID-19 in indoor places

4. RESULTS AND DISCUSSION

An algorithm for the simulation of the propagation of COVID-19 pandemic based the proposed model developed. Figure 4 in the previous section shows a flowchart plan of this algorithm which represents the rules of our proposed model. To begin with, the size of the matrix, the primary states of every CA cell, as well as the primary concentration of every state are read by the algorithm. These parameters can be proposed initially at shown in Table 1. Nevertheless, the CA cells are supposed to characterize the population as infected or susceptible. The range of each cell R is determined in conjunction with the nearest neighbor (N). Afterwards, the algorithm determines the ratio of infected individuals in all CA cells. Consequently, termination condition is applied. Usually, this condition is normally the completion of the amount of time generations identified by the user. The access time of every cell in the matrix is illustrated at the beginning of the time generation phase. This time is the assigned time for every cell randomly throughout every period indicating the beginning of the spreading process of COVID-19 from the cell to another cell throughout each time generation period. The access time designed for every cell differs from each successive time generation to another to satisfy the objectivity of the stochastic modeling technique. Therefore, in every time generation, the formation of the access time satisfies the transparency and fairness requirements for the simulation experiments.

4.1. Results with performance analysis

A number of simulation experiments were performed by MATLAB 2021 to predict the propagation pattern of COVID19 in bounded area. In the first case study, the author assumes one infected person cell (INF) transfers the virus agent through the whole cellular area such that the matrix of spreading is occupied by vacant cells or by susceptible cells (SUS) or cleared surface cells (CL). The initial conditions in the first experiment are shown in Table 1. The sample images of the population pattern with different species of population before and after dissemination produced by the proposed simulator are shown in Figure 5. Figure 5(a) presents population pattern with one infected person at the center of the area before virus propagation. Figure 5(b) presents the population pattern after virus propagation. Figure 6 shows the plot of population amount for various cellular species against the generation time.

Table 1. The initial conditions in the first experiment

Variable	Initial value
Matrix dimension	100x100
Initial number of holes	10% of cells
Initial number of surfaces contaminated with COVID-19(CO)	0
Initial number of people carry COVID-19(INF)	1
Start location of INF	(53,53)
Initial number of persons susceptible to COVID-19 (SUS)	45%
Initial number of surfaces cleared from COVID-19(CL)	45%
Time epochs	7

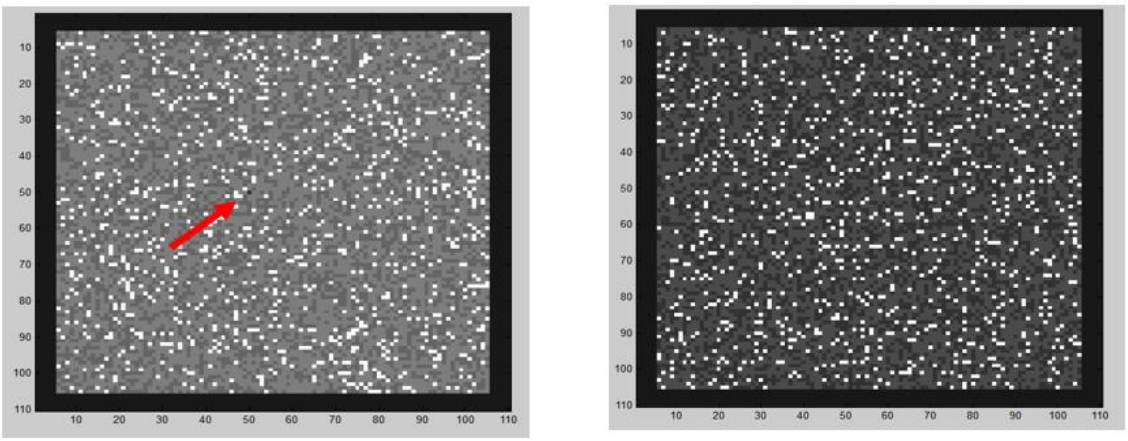

(a) (b)

Figure 5. Population pattern indicates different concentration of population before and after propagation. (a) one person carry COVID-19 at approximately the center of the matrix at time generation=0 before virus dissemination and (b) all persons and all surfaces carry COVID 19 at time generation=t_end. (White→holes, INF →ANCHOR, SUS→PEWTER, CL→STEEL, and CO→CHARCOAL)

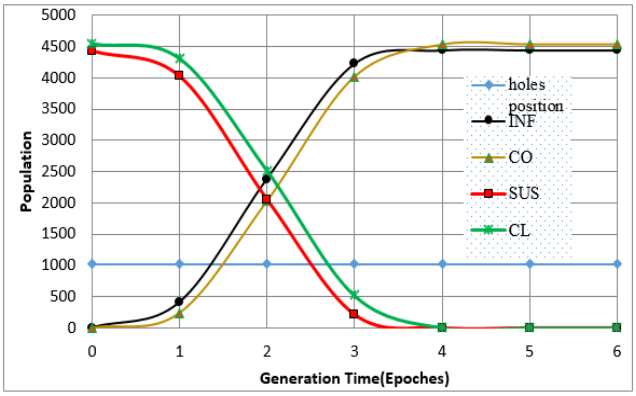

Figure 6. Generation time vs. population Amount for various cellular types

No variation was noticed if the initial pattern was one cellular surface (CO) in the center of the matrix. At this point the experimentation was extended to study the effect of variation of the percentage of cellular holes on the infected population (INF) pattern as shown in the Figure 7. It is notable that the percentage of holes is taken as 10%, 20%, and 30%. 40%, 1%, 3%, 5%, 7%, and 9% to show the infection pattern. Figure 7(a) shows, the infected population decreased with the increase in the percentage of holes for percentages greater than 10%. This shows the importance of increasing holes positions to decrease the percentage of the infected population. This pattern issues is different for holes percentages below 10% as shown in Figure 7(b). Figure 8 shows the shape of the population matrix produced by the simulator for holes with a concentration of 1%.

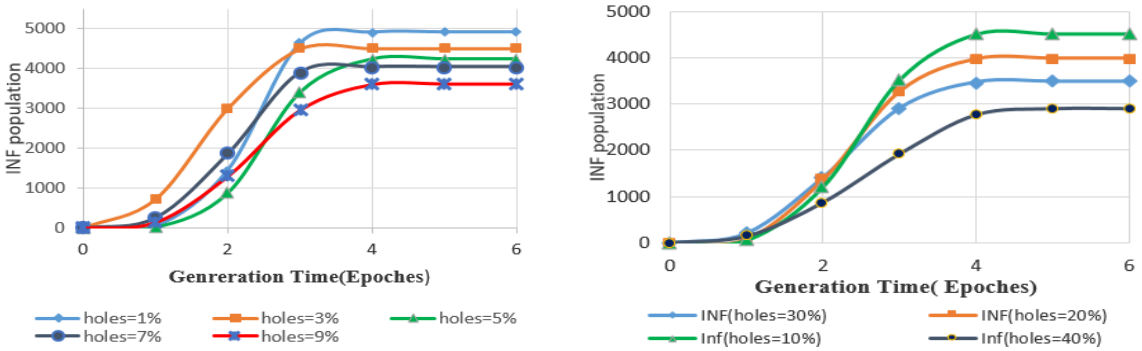

(a) (b)

Figure 7. Effects of variation of percentage of holes on the INF population for (a) percentages above 10% and (b) percentages less than 10%

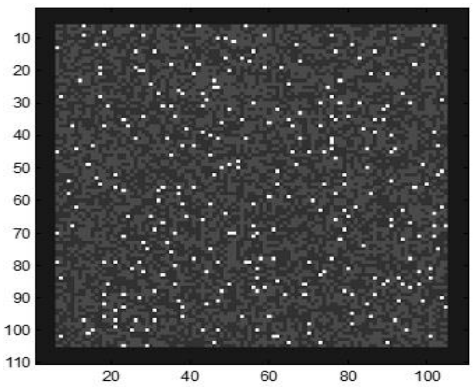

Figure 8. 1% of the locations are occupied by holes

The next case study assume the number about M^2 of infected personal cells (INF) such that M<<N concentrated at the center of the region and disseminate across the whole area with limited speed. Such that the matrix dominated by vacant cells or by susceptible cells (SUS) or cleared surface cells (CL). The dissemination simulation pattern is shown in Figure 9.

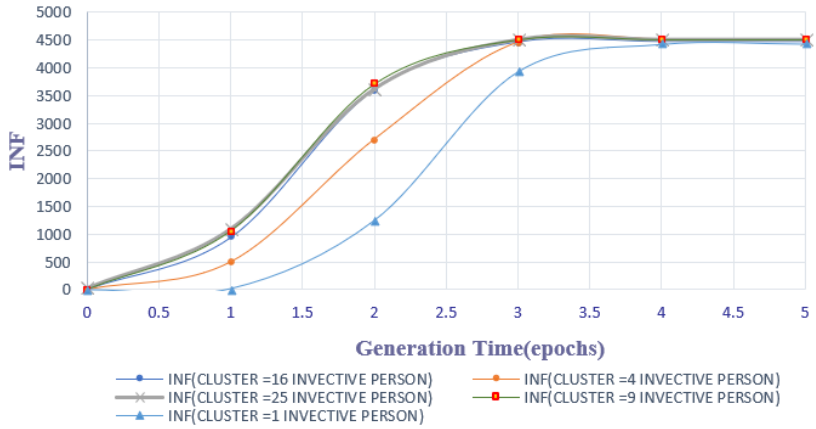

Figure 9. Shows how the size of the initial cluster of infected people affects the dissemination pattern

We noticed that the propagation patterns for the first three clusters with size 9, 16, 25 INF were nearly close to each other. Furthermore, the viral load is assessed throughout the area, and it is defined as the number of times each cell region is exposed to the Coronavirus carriers' infection. The cell region is assumed in our model to occupy an area of 50 m^2. The graph of viral load against region number is shown in Figure 10 under initial conditions of Table 1.

It should be noted that each epoch's time generation period is made up of a large number of viral spreading sessions for INF or CO cells, with each virus-spreading session lasting about one second. This is the time it takes for an illness to spread from an infected person to a cellular range or from a contaminated surface to a cellular range. The range of the INF cell was two meters whereas the range of the CO cell is half meter owing to contact probability. The real time is equivalent to the summation of all spreading sessions. Figure 11 indicates the population of all cellular species against real time in seconds. Further experiment, aims to study the effect of speed up of transfer of infective persons to holes positions on the dissemination pattern. The model assumes two rates of transfer for infected individuals 90% and 20%. The results are satisfactory and consistent with the clinical findings of the disease spread as shown in Figure 12.

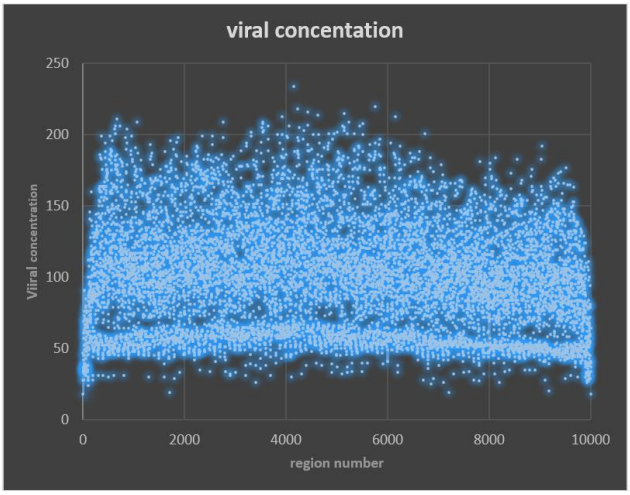

Figure 10. The load is raised in the middle regions because the initial infected person was localized in the middle of the squared area

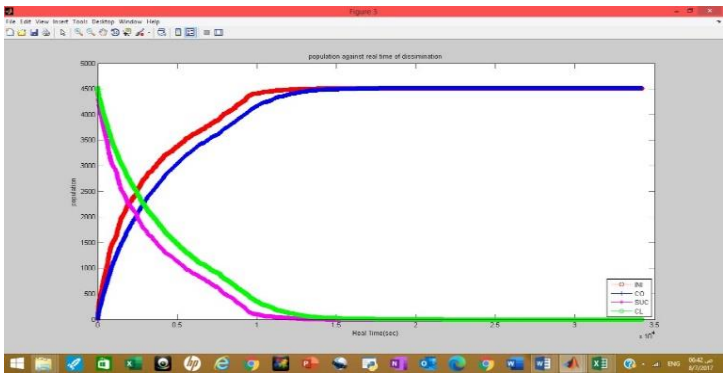

Figure 11. The population of all cellular species against real time in seconds

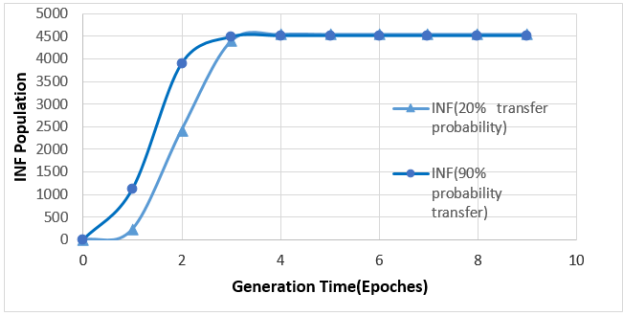

Figure 12. Effect of speed up of the population on the infective population

5. CONCLUSION

In this paper, a forecasting model based on a factual cellular automata approach is proposed and implemented with writing suitable MATLAB code to produce the proposed MAD-COV19 system simulator model. This model is largely based on formal empirical observations of spread of COVID-19 disease in indoor location based on the use of cellular automata techniques of thinking. Several experiments have been conducted on this model, which aims to track the percentage of people infected with time in different conditions and situations, as well as the percentage of contaminated surfaces over time. As well as tracking the infected cases over time with the change in the proportion of primary infected cases with the COVID-19 disease. The percentage of vacant places was also changed, and the extent of its impact on the spread of the disease was seen. A very fast spreading behavior was shown in the proposed area. This work may be considered a criterion for the propagation of COVID-19 in a defined population area. The propagation patterns for COVID-19 with our simulation model are compatible with theoretical background of SI model. The viral load is measured and explored in a specific area of a particular dimension. This paper also describes the model's dynamic mode. Infectious people's population is counted in a variety of ways. The population of polluted surfaces is also examined and evaluated. The overall technique and results are novel. A scenario where partly vaccinated individuals could be introduced in the population of susceptible individuals and should be considered in future work to make the model more realistic. In addition, further research is necessary on the utilization of big data collected on the COVID-19 pandemic in the future.

REFERENCES

[1] World Health Organisation, "Coronavirus disease (COVID-19) Weekly Epidemiological Update and Weekly Operational Update," 2020. [Online]. Available: https://www.who.int/emergencies/diseases/novel-coronavirus-2019/situation-reports

[2] V. C.-C. Cheng *et al.*, "Air and environmental sampling for SARS-CoV-2 around hospitalized patients with coronavirus disease 2019 (COVID-19)," *Infect. Control Hosp. Epidemiol.*, vol. 41, no. 11, pp. 1258–1265, Nov. 2020, doi: 10.1017/ice.2020.282.

[3] S. Barua, "Understanding coronanomics: the economic implications of the COVID-19 pandemic," *J. Dev. Areas*, vol. 55, no. 3, pp. 435–450, 2021, doi: 10.1353/jda.2021.0073.

[4] E. O. Nsoesie, R. J. Beckman, S. Shashaani, K. S. Nagaraj, and M. V. Marathe, "A simulation optimization approach to epidemic forecasting," *PLoS One*, vol. 8, no. 6, p. e67164, Jun. 2013, doi: 10.1371/journal.pone.0067164.

[5] W. Duan, Z. Fan, P. Zhang, G. Guo, and X. Qiu, "Mathematical and computational approaches to epidemic modeling: a comprehensive review," *Front. Comput. Sci.*, vol. 9, no. 5, pp. 806–826, Oct. 2015, doi: 10.1007/s11704-014-3369-2.

[6] H. Chen, W. Matthaeus, and L. Klein, "Theory of multicolor lattice gas: A cellular automaton poisson solver," *J. Comput. Phys.*, vol. 88, no. 2, pp. 433–466, Jun. 1990, doi: 10.1016/0021-9991(90)90188-7.
[7] I. Bialynicki-Birula, "Weyl, Dirac, and Maxwell equations on a lattice as unitary cellular automata," *Phys. Rev. D*, vol. 49, no. 12, pp. 6920–6927, Jun. 1994, doi: 10.1103/PhysRevD.49.6920.
[8] S. Athithan, V. P. Shukla, and S. R. Biradar, "Dynamic cellular automata based epidemic spread model for population in patches with movement," *J. Comput. Environ. Sci.*, vol. 2014, pp. 1–8, Feb. 2014, doi: 10.1155/2014/518053.
[9] E. Ahmed, H. N. Agiza, and S. Z. Hassan, "On modeling hepatitis B transmission using cellular automata," *J. Stat. Phys.*, vol. 92, no. 3–4, pp. 707–712, 1998, doi: 10.1023/a:1023001007714.
[10] T. Toffoli, "Cellular automata as an alternative to (rather than an approximation of) differential equations in modeling physics," *Phys. D Nonlinear Phenom.*, vol. 10, no. 1–2, pp. 117–127, Jan. 1984, doi: 10.1016/0167-2789(84)90254-9.
[11] W. Maniatty, B. Szymanski, and T. Caraco, "High-performance computing tools for modeling evolution in epidemics," in *Proceedings of the 32nd Annual Hawaii International Conference on Systems Sciences. 1999. HICSS-32. Abstracts and CD-ROM of Full Papers*, 1999, p. 10. doi: 10.1109/HICSS.1999.773085.
[12] A. Ilachinski, "Cellular automata: a discrete view. [Sl]." 2002.
[13] F. Brauer, "The Kermack-McKendrick epidemic model revisited," *Math. Biosci.*, vol. 198, no. 2, pp. 119–131, Dec. 2005, doi: 10.1016/j.mbs.2005.07.006.
[14] M. J. Keeling and L. Danon, "Mathematical modelling of infectious diseases," *Br. Med. Bull.*, vol. 92, no. 1, pp. 33–42, Dec. 2009, doi: 10.1093/bmb/ldp038.
[15] S. Ghosh and S. Bhattacharya, "Computational model on COVID-19 pandemic using probabilistic cellular automata," *SN Comput. Sci.*, vol. 2, no. 3, p. 230, May 2021, doi: 10.1007/s42979-021-00619-3.
[16] N. T. J. Bailey, *The mathematical theory of infectious diseases and its applications. 2nd edition.*, vol. 28, no. 2. Charles Griffin & Company Ltd, 5a Crendon Street, High Wycombe, Bucks HP13 6LE., 1975.
[17] L. J. S. Allen, "Some discrete-time SI, SIR, and SIS epidemic models," *Math. Biosci.*, vol. 124, no. 1, pp. 83–105, Nov. 1994, doi: 10.1016/0025-5564(94)90025-6.
[18] S. H. White, A. M. del Rey, and G. R. Sánchez, "Modeling epidemics using cellular automata," *Appl. Math. Comput.*, vol. 186, no. 1, pp. 193–202, Mar. 2007, doi: 10.1016/j.amc.2006.06.126.
[19] G. C. Sirakoulis, I. Karafyllidis, and A. Thanailakis, "A cellular automaton model for the effects of population movement and vaccination on epidemic propagation," *Ecol. Modell.*, vol. 133, no. 3, pp. 209–223, Sep. 2000, doi: 10.1016/S0304-3800(00)00294-5.
[20] M. Dascălu, M. Maliţa, A. Barbilian, E. Franţi, and G. M. Ştefan, "Enhanced cellular automata with autonomous agents for covid-19 pandemic modeling," *Rom. J. Inf. Sci. Technol.*, vol. 23, pp. S15–S27, 2020.
[21] J. Dai, C. Zhai, J. Ai, J. Ma, J. Wang, and W. Sun, "Modeling the Spread of Epidemics Based on Cellular Automata," *Processes*, vol. 9, no. 1, p. 55, Dec. 2020, doi: 10.3390/pr9010055.
[22] P. K. Jithesh, "A model based on cellular automata for investigating the impact of lockdown, migration and vaccination on COVID-19 dynamics," *Comput. Methods Programs Biomed.*, vol. 211, p. 106402, Nov. 2021, doi: 10.1016/j.cmpb.2021.106402.
[23] R. Cárdenas, K. Henares, C. Ruiz-Martín, and G. Wainer, "Cell-DEVS models for the spread of COVID-19," in *Lecture Notes in Computer Science (including subseries Lecture Notes in Artificial Intelligence and Lecture Notes in Bioinformatics)*, 2021, vol. 12599 LNCS, pp. 239–249. doi: 10.1007/978-3-030-69480-7_24.
[24] G. A. Wainer, "An introduction to cellular automata models with cell-DEVS," in *2019 Winter Simulation Conference (WSC)*, Dec. 2019, pp. 1534–1548. doi: 10.1109/WSC40007.2019.9004763.
[25] N. H. Packard and S. Wolfram, "Two-dimensional cellular automata," *J. Stat. Phys.*, vol. 38, no. 5–6, pp. 901–946, Mar. 1985, doi: 10.1007/BF01010423.

BIOGRAPHIES OF AUTHORS

Shahinaz M. Al-Tabbakh is a lecturer of computer sciences , computer sciences and applications group, Physics Department, Faculty of Women for Arts, Sciences and Education, Ain Shams University, Cairo, Egypt. She got a M.Sc. in Computer Modeling and simulation of a stochastic processes, Faculty of Women for Arts, sciences and Education, Ain Shams University, Egypt in 2001. She had a Ph. D in wireless mobile networking from Faculty of Women for Arts, sciences and education, Ain Shams University, Egypt, Novambere,2006. She contributed to a large number of papers in computer modeling, machine learning, IOT and Wireless networking that published internationally. She contributed to a number of local and international conferences. She is a member in IEEE Society. Her scope now is Computer Modelling, IOT, Wireless networks and Machine learning Models. She can be contacted at email: shahinaz.altabbakh@women.asu.edu.eg.

Marwa A. Karim is a lecturer of ophthalmology at the faculty of medicine Ain Shams University and Armed force medical college AFCM. She holds a Medical doctorate degree in ophthalmology and an ophthalmology fellowship of Royal college of surgeons Glasgow FRCS. She is a fellow of the international council of ophthalmology ICO, Cambridge USA. She is specialized in ophthalmic plastic surgery and specially interested in uveitis and Glaucoma. She is a member of the Egyptian ophthalmic society and Oculoplastic ophthalmic society of Egypt. She can be contacted at email: marwa_abdelkarim@med.asu.edu.eg.